Identification of Critical Spans for Monitoring Systems in Dynamic Thermal Rating

Marcelo Matus, *Member, IEEE*, Doris Sáez, *Senior Member, IEEE*, Mark Favley, Carlos Suazo-Martínez, José Moya, *Student Member, IEEE*, Guillermo Jiménez-Estévez, *Senior Member, IEEE*, Rodrigo Palma-Behnke, *Senior Member, IEEE*, Gabriel Olguín, *Member, IEEE*, and Pablo Jorquera

***Abstract*—Dynamic thermal rating (DTR) has been seen as an important tool for planning and operation of power systems, and recently, for smart-grid applications. To implement an effective DTR system, it is necessary to install monitoring stations along the studied lines, with a tradeoff between accurate estimations and equipment investments. In this paper, a novel heuristic is developed for identifying the number and locations of critical monitoring spans for the implementation of DTR. The heuristic is based on the use of historical-simulated weather data, obtained from a Mesoscale Weather Model, and the statistical analysis of the thermal capacities computed in each span along the line. The heuristic is applied to a line that is 325 km long in North Chile. Optimal monitoring sets, including the number and location of required monitoring stations, are determined for different confidence levels in all line segments. The results are compared to an equidistant monitoring strategy. The proposed heuristic shows robustness since it outperforms the equidistant monitoring strategy in all of the analyzed cases, especially for the longer line segments, which are subject to more complex weather patterns.**

***Index Terms*—Critical spans and hot-spot identification, dynamic thermal rating (DTR), smart grids, weather model applications in power systems.**

I. Introduction

SINCE THE first developments of real-time thermal rating systems for overhead transmission lines [1], dynamic thermal rating (DTR) has been seen as an important driver to improve the planning and operation of power systems. Today, DTR is also considered to be a fundamental tool in smart-grid applications [2].

The transmission capacity in overhead lines is typically limited by the conductor temperature effect in the sag clearance [3], which varies in time and along the line spans. This variability is mainly due to weather condition fluctuations [4], which are time and space dependent.

Manuscript received October 05, 2011; accepted January 03, 2012. Date of publication March 02, 2012; date of current version March 28, 2012. This work was supported by Transelec S.A. under the RET–University of Chile Academic Collaboration Agreement, and the CONICYT/BMBF Project 2009–165, RWTH Aachen, Germany. Paper no. TPWRD-00853-2011.

M. Matus, D. Sáez, C. Suazo-Martínez, J. Moya, G. Jiménez-Estévez, and R. Palma-Behnke are with the Center of Energy, Faculty of Mathematical and Physical Sciences, School of Engineering, University of Chile (CMM, ISCI, DIE), Chile.

M. Favley is with the Geophysics Department, Universidad de Chile, Santiago, Chile.

G. Olguín and P. Jorquera are with Transelec, Santiago, Chile.

Color versions of one or more of the figures in this paper are available online at http://ieeexplore.ieee.org.

Digital Object Identifier 10.1109/TPWRD.2012.2185254

Considering that weather conditions are not always possible to measure or to estimate, thermal line ratings have been traditionally computed using conservative assumptions. These ratings are then used by the Independent System Operator in the dispatch process independent of the actual meteorological conditions [5].

Usually, the use of these conservative assumptions may underestimate the line capacity and, in some cases, it may overestimate it, depending on the real characteristics and variability of the weather patterns to which the line is exposed [6].

During the last two decades, several methods and technologies have emerged, which enable real-time measurements of weather conditions and line operating parameters [7], making the use of DTR in the system operation and economic dispatch feasible, including online rating estimations and transmission capacity predictions [8]–[12].

Developments in DTR have also been used to reduce intervention in generation schedules [13], improve the utilization of remote generation facilities that may provide power at lower costs [14], enhance power system reliability, and support wind power integration [13], [15].

The theoretical determination of the line DTR requires obtaining the minimal value of the actual thermal capacities in all of the spans within the line [16]. However, monitoring the values for each span could be very expensive, impractical, or even impossible.

To implement a DTR system in an overhead line requires, at least, defining a monitoring strategy. It is critical to decide what to monitor, and the number of monitor stations and their locations, due to the existing trade off between accurate estimations and equipment investments, especially for long lines exposed to variable weather conditions.

There are several international examples of DTR applications. Some of them, for which the number of monitoring stations used is reported, are listed in Table I. However, in these reports there is not much information about the criteria used to determine the number of stations, nor the methodology applied to select their locations.

On the other hand, there are some studies which describe allocation strategies for monitoring stations. Black *et al.* [23] detailed the successful installation of DTR equipment by the Northern Ireland Electricity Company, which included measurement points located in low wind/sheltered areas that may experience the least cooling. In [24], monitor stations were located based on the manufacturer's engineering judgment and upon span orientation and wind sheltering. Pytlak and Musilek [25] indirectly consider the identification of hot spots,

TABLE I
EXAMPLES OF INTERNATIONAL EXPERIENCES DEPLOYING DTR SYSTEMS

Location	Company	Monitors	System	Reference
New Zealand	Transpower	2 tension	220 kV	[8], [17], [18]
Australia Tasmania	Transend	15 weather & 19 tension	110 kV	[17], [19]
USA California	PG&E	4 tension	230 kV	[7], [19]
USA Colorado	NCE	2 tension & 3 temperature	230 kV	[8]
USA W. Virginia	Virginia Power	5 tension	500 kV & 115 kV	[20]
USA S. Louisiana	Entergy	2 tension	230 kV	[20]
Brazil	CEMIG	6 temperature	138 kV	[21]
Chile	Pelambres	4 weather & 4 temperature	220 kV	[22]

which may be considered as possible locations for monitoring stations, based on weather model data analysis.

In this paper, a novel heuristic is presented for developing a monitoring strategy, including the definition of the number and location of the monitoring stations.

The proposed heuristic allows determining an optimal number and location of the monitoring stations, subject to the requirement of estimating the line thermal capacity with a given confidence value. These aspects comprise the main contribution of the proposed approach.

The heuristic is based on the use of weather model data. The main objective of the proposed heuristic is to determine an adequate number of monitoring stations required to estimate the DTR with a given confidence level, and to identify the corresponding monitoring station locations.

As a case study, the method was applied to a line 325 km long in North Chile, and compared to an equidistant monitoring strategy.

The results show the influence of the geographic and weather conditions in the DTR implementation, where coastal lines with high and uniform ventilation required a lower number of monitoring stations than inland lines with more variable weather patterns. Furthermore, the proposed heuristic shows robustness since it outperforms the equidistant monitoring strategy in all of the analyzed cases, especially for the longer line segments, which are also subject to more complex weather patterns.

II. PROPOSED HEURISTIC

The heuristic for determining an optimal number of and locations for the monitoring stations for a given confidence value is based on analysis of the thermal capacity that would be observed along the line over a relevant time period.

In this paper, historical series of the thermal capacities for each span within the line were computed from simulated weather conditions obtained from pre-existing weather model databases.

In this way, if the weather model data reproduces the dynamic of the weather conditions to which the line is exposed, it could be expected that the dynamic of the thermal capacities of the spans would also be properly characterized and represented.

In Sections III and IV, the weather model used, the dynamic thermal capacity determination, and the critical spans identification mechanism are presented. This comprises the proposed heuristic that determines the monitoring strategy, including the number and location of monitoring stations.

A. Weather Model

In coastal Central Chile, near-surface atmospheric circulations are strongly influenced by the local topography and the land-sea interface. This leads to spatiotemporal wind and temperature patterns that exhibit pronounced daily and seasonal cycles, and abrupt spatial decorrelation in transition regions (e.g., from coast to inland, or from high to low topography). Operational weather monitoring networks are widely spaced and cannot adequately capture this regional variability. Thus, the use of a global weather model is necessary to obtain realistic estimations of weather conditions along the power-line path analyzed.

In this study, the weather model conditions were generated with the Weather Research and Forecasting (WRF) [26], [27] mesoscale atmospheric model. WRF is a next-generation, limited area, nonhydrostatic modeling system, with terrain following eta-coordinate mesoscale designed to serve operational forecasting and atmospheric research needs.

The WRF provides a complete representation of the atmosphere in the sense that practically all key atmospheric processes that influence the weather are included in the model equations, as terms in the dynamic core of the model in its many physical parameterization schemes.

For the power line analyzed, in particular, the simulated historic weather conditions were computed from WRF pre-existing databases, which were generated to compose a wind energy atlas for central and Northern Chile [28]. This WRF database consists of simulations at 1-km resolution and 10-m vertical resolution.

The simulation period includes four separate months (January, April, July, and October) of a single year (2010). The months were chosen in order to obtain some degree of representation of the seasonal cycles.

For thermal capacity estimation, the relevant variables were saved at hourly intervals, including horizontal wind velocity vector components, ambient temperature, and solar radiation. These data were interpolated linearly to the midpoint of each span in the line. Wind velocity and temperature data were also interpolated vertically to a height of 16 m, which was the average height of the line conductor.

Among the meteorological variables that influence thermal capacity, wind speed has the greatest influence [12], [29]. Fig. 1 shows the map of average wind speeds in the study area.

The complexity of the simulated wind field is readily evident, and is characterized by strong winds along the coastal zone and a sharp decrease inland. As shown in Fig. 1, wind speeds generally remain strong day and night in the coastal region. In contrast, inland sites exhibit a clear afternoon maximum (related to strong surface heating during the day), but drop off considerably at other times.

For validation, the model data were compared with the stations that are part of local networks for air quality, agricultural,

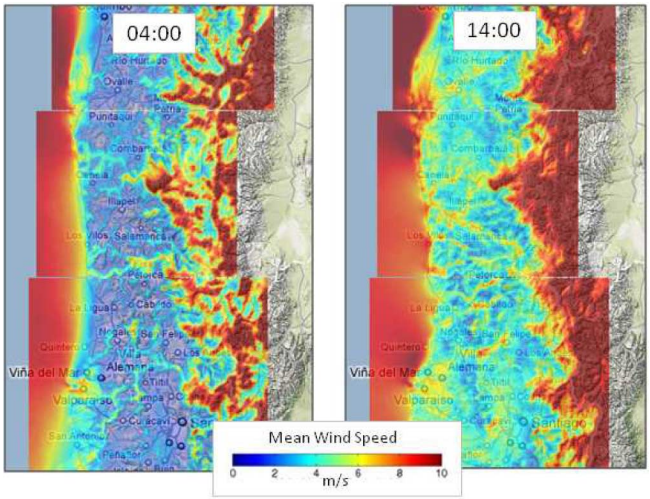

Fig. 1. Average wind speeds computed from the WRF model data.

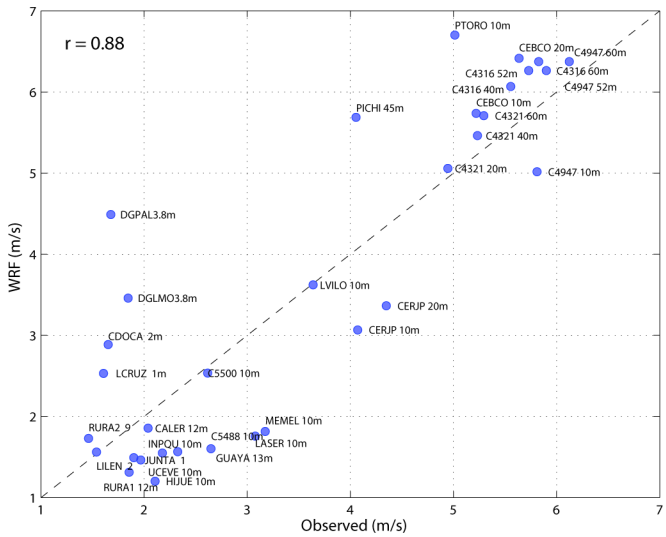

Fig. 2. Observed and modeled mean wind speeds at monitoring stations.

or wind energy monitoring. None of the stations are actually located along the transmission lines under study, but they are all fairly close (<20 km) and can be considered to be representative of model performance.

While there are no simultaneous meteorological observations available for the simulation time period, it is still possible to compare climatological statistics, such as mean wind speed and daily cycles. Fig. 2 shows a scatter plot of observed versus simulated mean wind speed. In the graph, the model values are averages of all hourly data over the four-month simulation period. Observed data are averaged over the period of data availability.

A strong correlation (0.88) can be seen between the data and the model. It is clearly possible to distinguish between areas of relatively high and low winds.

The differences between the observed wind speeds and the WRF's (which are considerable in a few cases) are likely due to the differences in the time periods examined, model biases, or problems in the observational data. It should be pointed out that many sites measure winds very close to the surface (10 m, or less in some cases), and these measurements may be affected by local site characteristics (vegetation, obstacles) that cannot be represented by the WRF model.

As can be seen in Fig. 1, the WRF simulations correctly capture the daily cycles at coastal and inland sites. Wind direction and temperature measures were also available at some sites. While the presentation of a detailed comparison of these variables is beyond the scope of this study, results indicate that the WRF model does well in predicting mean values and diurnal cycles of these variables also. Solar radiation observations were not available for comparison, but the influence of this variable on the thermal capacity variability is small [29].

B. Dynamic Thermal Capacity Determination

To capture the temporal and spatial variability of the weather conditions, the thermal capacity value is computed individually for each span of the line.

The thermal capacity is obtained from the thermodynamic heat balance of ohmic and solar heating against convective and radiative heat losses [7] using the steady-state thermal rating formula of the IEEE Standard 738-2006 [30]

$$C_i(t) = C_{\text{IEEE738}}(v_i(t), T_i(t), s_i(t), \vec{p_i}) \tag{1}$$

where

- $C_{\text{IEEE738}}(\cdot)$ is the steady-state thermal rating formula from the IEEE738 Standard;
- $v_i(t)$ is the representative wind speed in span i, including magnitude and direction, at instant t;
- $T_i(t)$ is the representative ambient temperature in span i at instant t;
- $s_i(t)$ is the representative solar radiation in span i at instant t;
- $\vec{p_i}$ is the set of the conductor and other nontemporal parameters in span i.

One of the relevant nontemporal parameters for the spans is the maximum temperature allowed T_C. In this study, T_C corresponds to the design temperature of the line. For this parameter, it is ensured that the minimum clearance according to local standards is satisfied in each span.

The thermal capacity for each span was computed hourly for the four months when the weather conditions were simulated. This is performed assuming that the weather variable values are representative of the given hour, and that the thermal steady state in the conductor has been reached. This is consistent with the expected transient times reported in [7] and [30].

Once the thermal capacity is computed for each span, the line dynamic thermal rating $C(t)$ is calculated as the minimum value observed through all spans. This means

$$C(t) = \min_{i \in S} C_i(t) \tag{2}$$

where S is the set of all span indices in the line.

C. Critical Spans Identification

As is shown in (2), to obtain the line DTR, the thermal capacities should be simultaneously calculated for all spans. On the other hand, to determine the line dynamic thermal rating with a given confidence level, it is only necessary to calculate a subset of thermal capacities for some critical spans.

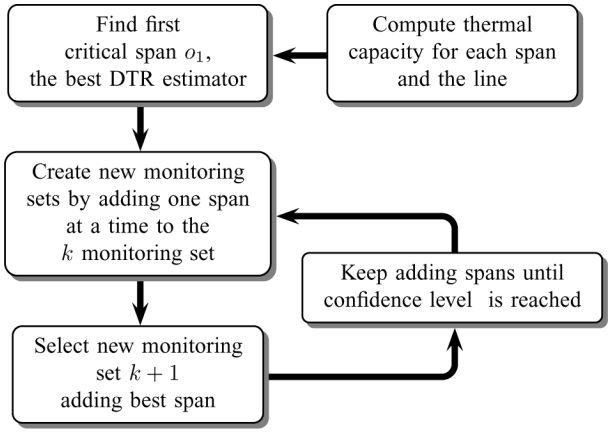

Fig. 3. Heuristic flow diagram.

In this study, the term "critical span" refers to the one that contributes relevant information for determining the global minimum and, therefore, a critical span is a good candidate for installing monitoring equipment capable of estimating the line DTR.

To determine these critical spans, an optimization problem can be formulated to select the minimal subset of spans that estimate the line DTR subject to a given confidence level. This formulation, however, requires solving an integer selection problem with nonpolynomial (NP) complexity in terms of the total and chosen number of spans, which may be impractical to solve.

To obtain a feasible and optimal solution in reasonable computational time, a heuristic is proposed, especially for long lines. As expected, there is no way to ensure that the optimal subset obtained from the heuristic is the global optimal for the original NP problem.

The applied criteria ensure that if the monitored span set is built by adding one chosen span at a time, the selected span maximizes the confidence level of the new monitored span set.

The iterative procedure of the heuristic is shown in Fig. 3. It starts computing the thermal capacity of each span and for the whole line, after which the first critical span is selected as the one which estimates the line DTR in the best way. From there, the set of critical spans is built by adding one span at a time, ensuring that the quality of the estimation of the line DTR is improved.

In this study, the quality of the estimation of the thermal capacity is measured using Pearson's correlation coefficient [31], which also provides the confidence level value of the estimation. Then, and according to Fig. 3, the first span to be selected is the one for which the correlation between its thermal capacity $C_i(t)$ and the line thermal capacity $C(t)$ is maximized

$$o_1 : \max_{o \in S} \operatorname{Corr}(C_o(t) C(t)) \tag{3}$$

where o_1 is the optimal index for the first span selected as the measuring point.

For short and very homogeneous lines, a single measuring point could be sufficient to estimate the line DTR, if the correlation value in (3) is reasonably close to 1. Nevertheless, in general, to reach an acceptable correlation value, the estimation of the line DTR may require more than one measuring point.

If more than one span is monitored, then the estimated value of the line thermal capacity at a given time is computed as the minimum of all the values observed, i.e.,

$$C_M(t) = \min_{j \in M} C_j(t) \tag{4}$$

where M is the set of indices of the monitored spans, which is a subset of S, and $C_M(t)$ is the estimated line thermal capacity value.

As before, the correlation between $C_M(t)$ and $C(t)$ quantifies how well the measuring set M can estimate the line thermal capacity. At the limit, when both sets M and S are identical, C_M and C are identical functions, and the correlation value is 1. Formally

$$\lim_{M \to S} \operatorname{Corr}(C_M(t), C(t)) = 1. \tag{5}$$

The selection of an optimal monitoring set M^* should maximize the correlation value in (5), for a given maximum cardinality

$$\begin{aligned} M_n^* : \max_{M \subset S} \quad & \operatorname{Corr}(C_M(t), C(t)) \\ \text{s.t.} \quad & |M| \leq n \end{aligned} \tag{6}$$

where $|M|$ represents the cardinality of the set M (i.e., the number of elements on it). Or, inversely, for a desired correlation value, the cardinality of the monitoring set M should be minimized

$$\begin{aligned} M_\rho^* : \min_{M \subset S} \quad & |M| \\ \text{s.t.} \quad & \operatorname{Corr}(C_M(t), C(t)) \geq \rho. \end{aligned} \tag{7}$$

Solving (7) directly is an $O\left(\binom{s}{n}\right)$ integer selection problem, where s is the total number of spans in the line, and n is the cardinality of the monitoring set.

Following the idea of the proposed heuristic, it is assumed that there is an optimal monitoring set M_k, with cardinality k, and it would be desirable to add a new monitoring span, with index o, forming in this way a new monitoring set M_{k+1}.

Formally, the new monitoring set is defined as the union of the previous set M_k and a new monitoring span with index o

$$M_{k+1}(o) = M_k \bigcup \{o\}. \tag{8}$$

Hence, there are $|S| - k$ possible new sets $M_{k+1}(o)$, including all of the spans that are not part of the M_k set. Using a similar criterion to the one applied to select the first critical span in (3), the optimal selection of the next critical span o_{k+1} should maximize the correlation between the line thermal capacity and the estimation of the next monitoring set

$$o_{k+1} : \max_{o \in S - M_k} \operatorname{Corr}(C_{M_{k+1}(o)}(t), C(t)) \tag{9}$$

where o_{k+1} is the optimal index of the next critical span and

$$M_{k+1} = M_k \bigcup \{o_{k+1}\} \tag{10}$$

is the next monitoring set.

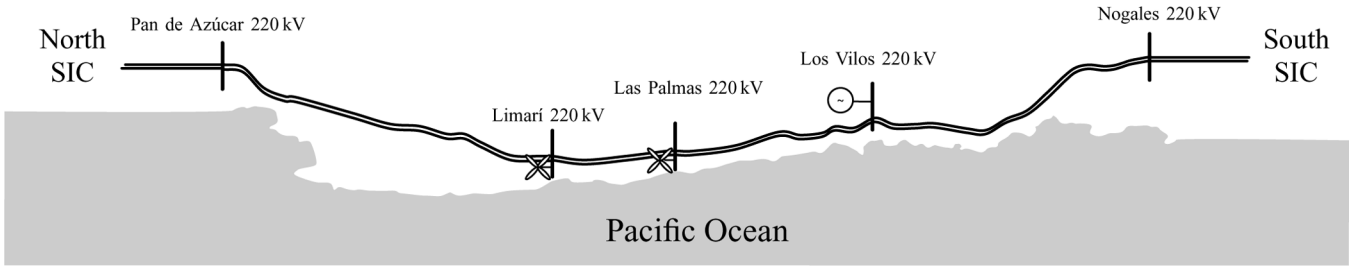

Fig. 4. Single-line diagram for the analyzed Nogales–Pan de Azúcar line, which interconnects the North and South SIC systems.

In short, the incremental heuristic proposed here selects new monitoring spans by maximizing the correlation of the resulting estimated thermal capacity from the expanded monitoring set and the line thermal capacity, starting with the selection of the first span as in (3) and following the process as in (9). This means that instead of solving the original $O\left(\binom{s}{n}\right)$ integer selection problem, n problems of order $O(s)$ need to be solved.

Since it is desirable to use the minimal number of monitoring spans, the process will be stopped when the correlation value between the estimated value from the monitoring set $C_{M_{k+1}}(t)$ and the thermal capacity computed for the line $C(t)$ reaches the desired confidence value.

III. Case Study

The line "Nogales–Pan de Azúcar" (NPDA) included in this study is located in North Central Chile, and is part of the Chilean Interconnected Power System (SIC). It is 325 km long. Four wind farms are connected (Canela I, Canela II, Totoral, and Monte Redondo) to busbars Limarí 220 kV and Las Palmas 220 kV, with a total installed capacity of 164 MW, and with expected expansions in the near future of up to 300 MW.

Fig. 4 shows the simplified unilineal diagram for the NPDA line. As can be observed, two segments of the line are located inland (near busbar Pan de Azúcar 220 kV and Nogales 220 kV), and the main part of the line is located near the coast, which causes the analysis of the entire line to be done in four distinctive transmission segments.

In all four transmission segments, the heuristic for identifying the critical spans, described in the previous section, was applied.

For comparison, an equidistant monitoring placement strategy was also applied to the NPDA line. This strategy is included as a simple benchmark in this paper since in the absence of any other criteria, equidistant monitoring placement is, in general and in many fields, the selected approach to follow. This could be the case, for example, when the information about the line weather conditions, where DLR would be applied, is simply not available or is inadequate.

A. Equidistant Monitoring Placement Strategy

When the equidistant placement strategy is applied, for a given number of monitoring spans, a monitoring set E_n is built choosing n span indices equally spaced by $|S| - 1/n + 1$.

Fig. 5 shows the correlation values between thermal capacity of different segments and the estimated capacity from the E_n monitoring sets, as a function of the number of monitoring stations corresponding to the cardinality of the monitoring sets E_n.

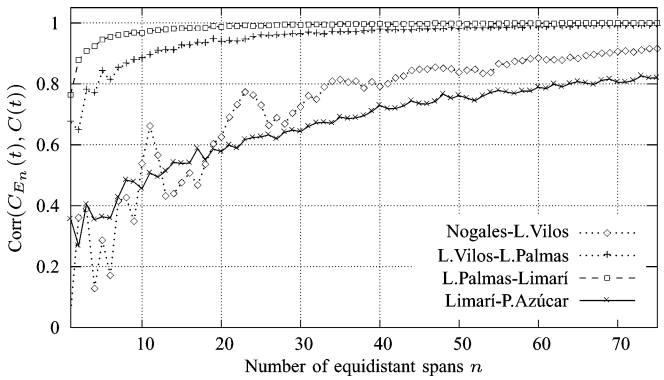

Fig. 5. Thermal capacity correlations for equidistant placement strategy.

As observed from Fig. 5, the correlation values reached with a given number of monitoring spans for the shorter coastal segments (Los Vilos–Las Palmas 220 kV and Las Palmas–Limarí 220 kV) are much higher than for the longer inland ones (Nogales–Los Vilos 220 kV and Limarí–Pan de Azúcar 220 kV).

As shown in Fig. 5, inland lines exhibit nonmonotonic behavior. Increasing the number of monitoring spans does not always increase the correlation value of the resulting monitoring set. Thus, a small number of monitoring stations may estimate the line thermal capacity better than a monitoring set with larger cardinality.

This effect is more exacerbated when a reduced number of monitoring stations is available. This reveals the importance of choosing the correct monitoring locations, for a better estimation of hot-spots within the line.

The nonmonotonic behavior can be explained by the fact that by increasing the cardinality of the monitoring set, from k to $k+1$, the resulting monitoring set E_{k+1} will be different from the previous E_k monitoring set. And if in the set E_k there were some critical or hot-spot locations, the next set E_{k+1}, by using a different separation between spans, may miss them.

When the cardinality of the monitoring set gets large enough, the nonmonotonic effects tend to disappear, and there is a small gain in the correlation values obtained for the larger monitoring sets.

The effectiveness of the equidistant strategy may be acceptable for short lines with uniform weather patterns, such as the coastal lines. But for long lines with more variable weather conditions, such as those inland, the equidistant location strategy may be impractical or at least very expensive to implement.

TABLE II
EQUIDISTANT MONITORING STATIONS NEEDED FOR DIFFERENT ρ

	Total	$\rho = 0.85$		$\rho = 0.90$		$\rho = 0.95$	
Segment	Spans	Stations	Ratio	Stations	Ratio	Stations	Ratio
Nogales - L.Vilos	248	54	16.9%	68	27.4%	110	44.3%
L.Vilos - L.Palmas	197	8	4.1%	12	6.1%	23	11.6%
L.Palmas - Limarí	67	2	3.0%	3	4.5%	6	9.0%
Limarí - P.Azúcar	339	87	25.7%	141	41.6%	274	80.8%
Total	851	151	17.7%	224	26.3%	413	48.5%

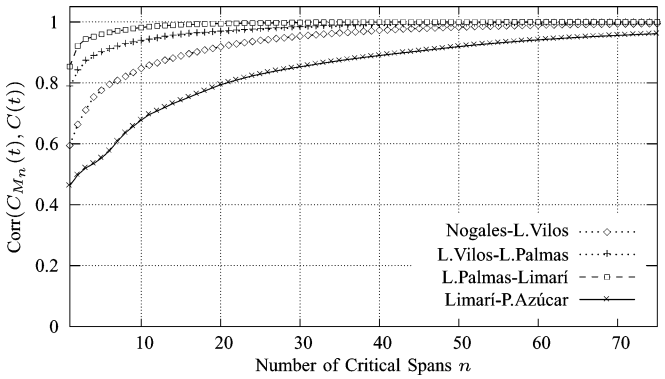

Fig. 6. Thermal capacity correlations for the critical span monitoring strategy.

Table II describes the total number of monitoring stations needed for a given confidence level in each segment (Stations column) and indicates the ratio between the monitored spans and total spans (Ratio column). In fact, as presented in Table II, to reach a reasonable confidence value of 0.9 in the two coastal segments (Los Vilos–Las Palmas 220 kV and Las Palmas–Limarí 220 kV) 12 and 3 monitor stations are needed, respectively. In contrast, for the two inland segments (Nogales–Los Vilos 220 kV and Limarí–Pan de Azúcar 220 kV), to reach the same confidence levels, up to 68 and 141 monitors are needed, respectively. For a confidence level of 0.95, the difference in the cardinality of the monitoring sets is even greater.

B. Critical Span Monitoring Strategy

Fig. 6 shows the correlation between the thermal capacity of each segment and the capacity estimated by the proposed heuristic in Section II, as a function of the number of monitoring stations located following the heuristic. The monotonic behavior for the four segments can be observed. Thus, the monitoring set estimation confidence improves as the number of monitoring sets are constructed and the number of spans in them is increased. This effect is more pronounced in the inland segments, which, as previously described, are longer and subject to more variable weather patterns then the coastal ones.

Table III describes the total number of monitoring stations needed for a given confidence level and indicates the ratio between the monitored spans and the total spans. As shown, the number of critical spans is larger for the longer segments (Limarí–Pan de Azúcar 220 kV and Nogales–Los Vilos 220 kV). In this case, inland segments are the most complex parts of the line to monitor given the more variable weather conditions. Contrarily, due to the short length of the coastal segments, coupled with stable weather conditions in the region, it is possible to determine thermal capacity with the same confidence level by using a smaller number of monitoring stations.

TABLE III
CRITICAL MONITORING STATIONS NEEDED FOR DIFFERENT ρ

	Total	$\rho = 0.85$		$\rho = 0.90$		$\rho = 0.95$	
Segment	Spans	Stations	Ratio	Stations	Ratio	Stations	Ratio
Nogales - L.Vilos	248	11	4.4%	17	6.9%	29	11.6%
L.Vilos - L.Palmas	197	3	1.5%	6	3.0%	14	7.1%
L.Palmas - Limarí	67	1	1.5%	2	3.0%	4	6.0%
Limarí - P.Azúcar	339	30	8.8%	44	13.0%	66	19.5%
Total	851	45	5.3%	69	8.1%	113	13.3%

In addition to the number of critical spans, the proposed heuristic also determines their locations. For example, in the case of the shorter line, Los Vilos–Las Palmas 220 kV, for a confidence level of 0.9 (see Table III), the six critical spans that were identified correspond to spans 10, 21, 29, 63, 127, and 193. In the case of the segment Las Palmas–Limarí- 220 kV, to reach the same confidence level, the two monitoring stations are strategically located at spans 8 and 54.

C. Discussion

When the equidistant monitoring strategy results are compared to those of the proposed heuristic, the most notable difference is their marked nonmonotonic and monotonic behavior, especially for the inland segments, as shown in Figs. 5 and 6.

As mentioned before, the nonmonotonic behavior observed for the equidistant monitoring strategy can be explained by the fact that between consecutive monitoring sets E_k and E_{k+1}, there are no common spans. On the other hand, for the proposed heuristic, the monotonic behavior is ensured by construction, since the monitoring sets are built by adding one new span at a time, and preserving all of the previous ones. In this case, increasing the cardinality always increases the information in the set, and the quality of the line thermal capacity estimation.

By comparing Tables II and III, it is also clear that for the given correlation values, the proposed heuristic always requires fewer monitoring stations, especially for the inland segments. For example, in the extreme case of the Limarí–Pan de Azúcar 220-kV segment, to reach a 0.95 confidence level, the equidistant monitoring strategy requires 274 instrument spans while with the proposed heuristic, only 66 monitoring stations are needed.

This dramatic reduction is due to the proper identification of the critical spans and the corresponding location of the monitoring stations.

The proposed heuristic also shows better performance since, as can be seen in Fig. 6, it has faster convergence to the asymptotic value of 1.

IV. CONCLUSION

A novel heuristic was developed to identify an optimal monitoring span set for dynamic line rating, including both, an optimal number, and optimal locations of the critical spans, which are required to instrument and monitor.

The heuristic is based on the use of historical simulated data obtained from a Mesoscale Weather Model, iteratively identifying the critical spans required to estimate the line thermal capacity with a given confidence level. The iterative nature of the heuristic enables progressive implementation and verification of the monitoring strategy.

The complexity of the heuristic presented is $O(s \times n)$, where s is the total number of spans in the line and n is the number of selected monitored spans. This makes the heuristic feasible and practical to use even for long lines, and contrasts with the original integer selection problem complexity of $O\left(\binom{s}{n}\right)$.

The heuristic was applied to the four segments of the Nogales–Pan de Azúcar transmission line in Chile (with a total of 851 spans and 325 km long), and showed robustness since it outperformed the equidistant monitoring strategy in all cases analyzed, especially for the longer line segments, which are subject to more variable weather patterns.

The heuristic shows desired monotonic behavior in terms of the number of monitoring spans and the confidence level reached in the estimation of the line thermal capacity. This means that the quality of the line thermal rating estimation always increased as the number of monitoring spans increased.

On the other hand, in some cases, and especially for long lines, the equidistant monitoring strategy may lead to a contradictory situation, where by considering more monitoring stations, the quality of the line thermal capacity estimation worsens.

The analysis of the proposed heuristic and the equidistant monitoring strategy reveals the importance of properly defining a monitoring strategy when designing a dynamic thermal rating system.

This work also reveals the role and relevance of weather models and statistical analysis of the weather patterns in the planning, scheduling, and operation of power systems.

ACKNOWLEDGMENT

The authors would like to thank U. Soto and R. Alvarez for their help and discussions during this study.

REFERENCES

[1] M. W. Davis, "A new thermal rating approach: The real time thermal rating system for strategic overhead conductor transmission lines part IV daily comparisons of real-time and conventional thermal rating and establishment of typical annual weather models," *IEEE Trans. Power App. Syst.*, vol. PAS-99, no. 6, pp. 2184–2192, Nov. 1980.

[2] A. K. Kazerooni and J. Mutale, "Dynamic thermal rating application to facilitate wind energy integration," presented at the IEEE Power Eng. Soc. Trondheim, Trondheim, Norway, 2011, IEEE Norwegian Univ. Sci. Technol.

[3] D. A. Douglass and A. A. Edris, "Field studies of dynamic thermal rating methods for overhead lines," in *Proc. IEEE Transm. Distrib. Conf.*, Apr. 1999, vol. 2, pp. 842–851.

[4] D. A. Douglass, "Weather-dependent versus static thermal line ratings [power overhead lines]," *IEEE Trans. Power Del.*, vol. 3, no. 2, pp. 742–753, Apr. 1988.

[5] J. Fu, S. Abbott, B. Fox, D. J. Morrow, and S. Abdelkader, "Wind cooling effect on dynamic overhead line ratings," in *Proc. 45th Int. Univ. Power Eng. Conf.* , Sep. 31, 2010, pp. 1–6.

[6] S.-H. Huang, W.-J. Lee, and M.-T. Kuo, "An online dynamic cable rating system for an industrial power plant in the restructured electric market," *IEEE Trans. Ind. Appl.*, vol. 43, no. 6, pp. 1449–1458, Nov./Dec. 2007.

[7] R. Adapa and D. A. Douglass, "Dynamic thermal ratings: Monitors and calculation methods," in *Proc. IEEE Power Eng. Soc. Inaugural Conf. Expo. Africa*, Jul. 2005, pp. 163–167.

[8] T. O. Seppa, S. Damsgaard-Mikkelsen, M. Clements, R. Payne, and N. Coad, "Application of real time thermal ratings for optimizing transmission line investment and operating decisions," presented at the CIGRE, Paris, France, 2000.

[9] Y. Yang, R. Harley, D. Divan, and T. Habetler, "Adaptive Echo state network to maximize overhead power line dynamic thermal rating," in *Proc. IEEE Energy Convers. Congr. Expo.*, Sep. 2009, pp. 2247–2254.

[10] Y. Yang, D. Divan, R. Harley, and T. Habetler, "Real-time dynamic thermal rating evaluation of overhead power lines based on online adaptation of Echo state networks," in *Proc. IEEE Energy Convers. Congr. Expo.*, Sep. 2010, pp. 3638–3645.

[11] O. Ciniglio and A. Deb, "Optimizing transmission path utilization in Idaho power," *IEEE Trans. Power Del.*, vol. 19, no. 2, pp. 830–834, Apr. 2004.

[12] D.-M. Kim, J.-M. Cho, H.-S. Lee, H.-S. Jung, and J.-O. Kim, "Prediction of dynamic line rating based on assessment risk by time series weather model," in *Proc. Int. Conf. Probab. Meth. Appl. Power Syst.*, Jun. 2006, pp. 1–7.

[13] T. Ringelband, M. Lange, M. Dietrich, and H. J. Haubrich, "Potential of improved wind integration by dynamic thermal rating of overhead lines," in *Proc. IEEE Bucharest PowerTech*, Jul. 28, 2009, pp. 1–5.

[14] M. Khaki, P. Musilek, J. Heckenbergerova, and D. Koval, "Electric power system cost/loss optimization using dynamic thermal rating and linear programming," in *Proc. IEEE Elect. Power Energy Conf.*, Aug. 2010, pp. 1–6.

[15] T. Yip, C. An, G. Lloyd, M. Aten, and B. Ferri, "Dynamic line rating protection for wind farm connections," in *Proc. CIGRE/IEEE PES Joint Symp. Integr. Wide-Scale Renew. Resources Into Power Del. Syst.,* , Jul. 2009, pp. 1–5.

[16] L. Ren, X. Jiang, G. Sheng, and W. Bo, "Design and calculation method for dynamic increasing transmission line capacity," *WSEAS Trans. Circuits Syst*, vol. 7, pp. 348–357, May 2008.

[17] H. T. Consulting, Dynamic transmission line rating technology review Cambridge, Tasmania, Australia, 2009. [Online]. Available: www.ea.govt.nz/document/3677/download/industry/ec.../tter-phase-2/

[18] J. K. Raniga and R. K. Rayudu, "Dynamic rating of transmission lines-a New Zealand experience," in *Proc. IEEE Power Eng. Soc. Winter Meeting*, 2000, vol. 4, pp. 2403–2409.

[19] T. O. Seppa, "Increasing transmission capacity by real time monitoring," in *Proc. IEEE Power Eng. Soc. Winter Meeting*, 2002, vol. 2, pp. 1208–1211.

[20] T. O. Seppa, H. W. J. Adams, D. A. Douglass, N. Coad, A. Edris, P. Olivier, and F. R. J. Thrash, "Use of on-line tension monitoring for real-time thermal ratings, ice loads, and other environmental effects," in *Proc. CIGRE Meeting*, Paris, France, 1998, pp. 1–5.

[21] C. Nascimento, J. Brito, E. Filho, G. Braga, G. Miranda, A. Bracarense, and S. Ueda, "The state of the art for increased overhead line ampacity utilizing new technologies and statistical criteria," in *Proc. IEEE/Power Eng. Soc. Transm. Distrib. Conf. Expo.: Latin America*, Nov. 2004, pp. 464–464.

[22] M. Pavez, Monitoreo dinámico en líneas de AT ExpoEnergia 2009, Santiago, Chile, 2009. [Online]. Available: http://www.microbyte.cl/elec/expo/2009energia/soltex.pdf

[23] J. Black, S. Connor, and J. Colandairaj, "Planning network reinforcements with dynamic line ratings for overhead transmission lines," in *Proc. 45th Int. Univ. Power Eng. Conf.*, Sep. 31, 2010, pp. 1–6.

[24] P. M. Callahan and D. A. Douglass, "An experimental evaluation of a thermal line uprating by conductor temperature and weather monitoring," *IEEE Trans. Power Del.*, vol. 3, no. 4, pp. 1960–1967, Oct. 1988.

[25] P. Pytlak and P. Musilek, "An intelligent weather-based system to support optimal routing of power transmission lines," in *Proc. IEEE Elect. Power Energy Conf.*, Aug. 2010, pp. 1–6.

[26] J. Michalakes, S. Chen, J. Dudhia, L. Hart, J. Klemp, J. Middlecoff, and W. Skamarock, "Development of a next generation regional weather research and forecast model," *Math. Comput. Sci.*, 2001.

[27] J. Michalakes, J. Dudhia, D. Gill, T. Henderson, J. Klemp, W. Skamarock, and W. Wang, W. Zwieflhofer and G. Mozdzynski, Eds., "The weather research and forecast model: Software architecture and performance," in *Proc. Use High Perf. Comput. Meteorol.*, Reading, U.K., 2004, pp. 156–168.

[28] Comisión Nacional de Energía, "Modelación del Recurso Solar y Eólico en el Norte de Chile," elaborated by Dept. Geofísica de la Universidad de Chile, Tech. Rep., 2009.

[29] G. M. L. M. van de Wiel, "A new probabilistic approach to thermal rating overhead line conductors evaluation in the Netherlands," in *Proc. Int. Conf. Overhead Line Design and Construction: Theory and Practice*, Nov. 1988, pp. 17–21.
[30] *IEEE Standard for Calculating the Current-Temperature of Bare Overhead Conductors*, IEEE Standard 738-2006, 2007, Revision of IEEE Standard 738-1993.
[31] J. L. Rodgers and W. A. Nicewander, "Thirteen ways to look at the correlation coefficient," in *American Stat.*, 1988, vol. 42, pp. 59–59. [Online]. Available: http://www.jstor.org/stable/2685263?origin=crossref

Marcelo Matus (M'10) received the B.Sc. and M.Sc. degrees in electrical engineering from the Pontificia Universidad Católica de Chile, Santiago, and the Ph.D. degree in electrical and computational sciences from the University of Tucson, Tucson, AZ, in 2005.

Currently, he is a Research Associate with the Center of Energy, Faculty of Mathematical and Physical Sciences, University of Chile, Santiago. His research fields are the planning and operational research of electrical systems and complex systems.

Doris Sáez (SM'05) received the M.Sc. and Ph.D. degrees in electrical engineering from the Pontificia Universidad Católica de Chile, Santiago, in 1995 and 2000, respectively.

Currently, she is an Associate Professor in the Electrical Engineering Department, University of Chile, Santiago, and collaborates with the Center of Energy, Faculty of Mathematical and Physical Sciences, University of Chile. Her research fields are fuzzy systems control design, fuzzy identification, predictive control, control of power generation plants, and control of transport systems.

Mark Favley received the B.Sc. and Ph.D. degrees in geophysics from the Victoria University of Wellington, Wellington, New Zealand, in 1997 and 2003, respectively.

Currently, he is a Research Associate with the Geophysical Department, University of Chile, Santiago. His research fields are atmospheric processes in complex terrain and numerical modeling of the atmosphere.

Carlos Suazo-Martínez received the B.Sc. and M.Sc. degrees in electrical engineering from the University of Chile, Santiago, in 2009.

Currently, he is a Research Associate with the Center of Energy, Faculty of Mathematical and Physical Sciences, University of Chile. His research interests are the analysis, operation, and control of electrical systems in competitive power markets, and optimization methods applied to electrical systems and power markets.

José Moya (S'11) received the B.Sc. degree in electrical engineering from the University of Chile, Santiago, in 2011.

His main research interest is the planning and operation of energy systems.

Guillermo Jiménez-Estévez (SM'11) received the B.Sc. degree in electrical engineering from the Escuela Colombiana de Ingeniería, Bogotá, Colombia, in 1998, and the M.Sc. and Ph.D. degrees in electrical engineering from the Universidad de Chile, Santiago, in 2003 and 2010, respectively.

Currently, he is a Research Associate with the Center of Energy, Faculty of Mathematical and Physical Sciences, University of Chile. His main research interests are distributed generation and distribution systems planning.

Rodrigo Palma-Behnke (SM'04) received the B.Sc. and M.Sc. degrees in electrical engineering from the Pontificia Universidad Católica de Chile, Santiago, in 1994, and the Dr.-Eng. degree from the University of Dortmund, Dortmund, Germany, in 1999.

Currently, he is a Professor in the Electrical Engineering Department, University of Chile, Santiago, and Director of the Center of Energy, Faculty of Mathematical and Physical Sciences, University of Chile. His research field is the planning and operation of electrical systems in competitive power markets and new technologies.

Gabriel Olguín (M'05) received the B.Sc. degree in electrical engineering from the University of Santiago Chile, Santiago, in 1993, the M.Sc. degree in power engineering from the Federal University of Santa Catarina, Florianopolis, Brazil, in 1999, and the Ph.D. degree in power engineering from Chalmers University of Technology, Gothenburg, Sweden, in 2005.

Currently, he is Technology Manager with Transelec S.A., Santiago, Chile, and an Assistant Professor at the University of Santiago.

Mr. Olguín is a certified Power Engineer from the University of Santiago.

Pablo Jorquera received the B.Sc. degree in 2009.

Currently, he is a Study Engineer with Transelec S.A., Santiago, Chile, in the New Technologies Unit, which supports the incorporation of flexible ac transmission systems technology into the main grid. He works on the design of HVDC projects in Southern Chile.

Mr. Jorquera is a certified Power Engineer from the University of Santiago.